J. Pharm. Pharmacol. 1998, 50: 265–274
Received September 5, 1997
Accepted November 26, 1997

Kinetic Characterization and Identification of the Enzymes Responsible for the Hepatic Biotransformation of Adinazolam and *N*-Desmethyladinazolam in Man

KARTHIK VENKATAKRISHNAN, LISA L. VON MOLTKE, SU XIANG DUAN, JOSEPH C. FLEISHAKER*, RICHARD I. SHADER AND DAVID J. GREENBLATT

*Department of Pharmacology and Experimental Therapeutics, Tufts University School of Medicine, and the Division of Clinical Pharmacology, New England Medical Center Hospital, Boston, MA and *The Clinical Pharmacokinetics Unit, Pharmacia and Upjohn, Kalamazoo, MI, USA*

Abstract

The kinetics of the *N*-demethylation of adinazolam to *N*-desmethyladinazolam (NDMAD), and of NDMAD to didesmethyladinazolam (DDMAD), were studied with human liver microsomes using substrate concentrations in the range 10–1000 μM. The specific cytochrome P450 (CYP) isoforms mediating the biotransformations were identified using microsomes containing specific recombinant CYP isozymes expressed in human lymphoblastoid cells, and by the use of CYP isoform-selective chemical inhibitors.

Adinazolam was demethylated by human liver microsomes to NDMAD, and NDMAD was demethylated to DDMAD; the substrate concentrations, K_m, at which the reaction velocities were 50% of the maximum were 92 and 259 μM, respectively. Another metabolite of yet undetermined identity (U) was also formed from NDMAD (K_m 498 μM). Adinazolam was demethylated by cDNA-expressed CYP 2C19 (K_m 39 μM) and CYP 3A4 (K_m 83 μM); no detectable activity was observed for CYPs 1A2, 2C9, 2D6 and 2E1. Ketoconazole, a relatively specific CYP 3A4 inhibitor, inhibited the reaction; the concentration resulting in 50% of maximum inhibition, IC50, was 0·15 μM and the inhibition constant, K_i, was $< 0{\cdot}04$ μM in five of six livers tested. Troleandomycin, a specific inhibitor of CYP 3A4, inhibited adinazolam *N*-demethylation with an IC50 of 1·96 μM. The CYP 2C19-inhibitor omeprazole resulted in only partial inhibition (IC50 21 μM) and sulphaphenazole, α-naphthoflavone, quinidine and diethyldithiocarbamate did not inhibit the reaction. NDMAD was demethylated by cDNA-expressed CYP 3A4 (K_m 220 μM, Hill number A 1·21), CYP 2C19 (K_m 187 μM, Hill number A 1·29) and CYP 2C9 (K_m 1068 μM). Formation of U was catalysed by CYP 3A4 alone. Ketoconazole strongly inhibited NDMAD demethylation (IC50 0·14 μM) and formation of U (IC50 $< 0{\cdot}1$ μM) whereas omeprazole and sulphaphenazole had no effect on reaction rates.

These results show that CYP 3A4 is the primary hepatic CYP isoform mediating the *N*-demethylation of adinazolam and NDMAD. Co-administration of adinazolam with CYP 3A4 inhibitors such as ketoconazole or erythromycin might lead to reduced efficacy, since adinazolam by itself has relatively weak benzodiazepine agonist activity, with much of the pharmacological activity of adinazolam being attributable to its active metabolite NDMAD.

Adinazolam (Figure 1) is a triazolobenzodiazepine that has been studied for the treatment of depression, panic disorder and general anxiety. After oral administration to man adinazolam undergoes extensive pre-systemic extraction to form an active metabolite, *N*-desmethyladinazolam (NDMAD) (Figure 1). Values of area under the plasma concentration–time curve for NDMAD are 2 to 5 times higher than those for adinazolam (Fleishaker & Phillips 1989).

In-vitro, adinazolam and NDMAD both bind to central benzodiazepine receptors, but NDMAD has

Correspondence: D. J. Greenblatt, Department of Pharmacology and Experimental Therapeutics, Tufts University School of Medicine, 136 Harrison Avenue, Boston, MA 02111, USA.

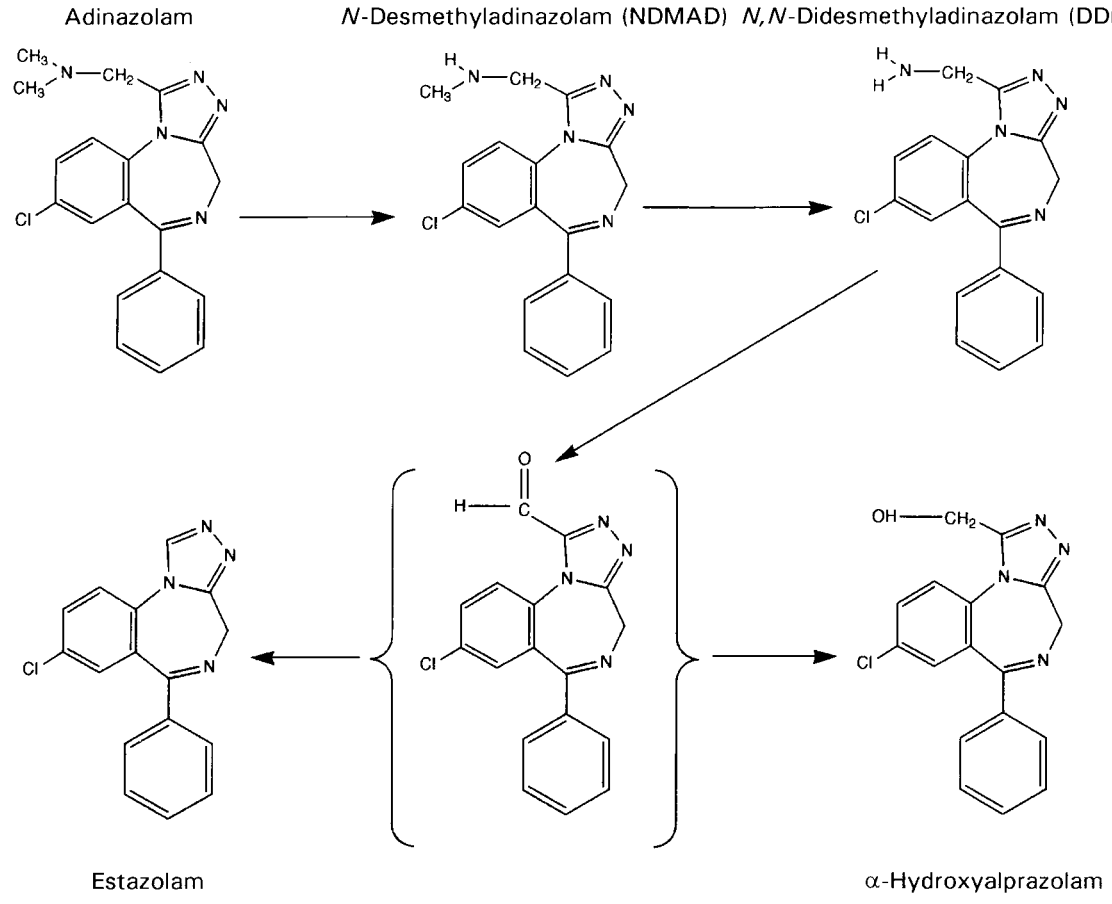

Figure 1. The chemical structures and biotransformation pathways of adinazolam and its metabolites.

approximately 25-fold higher affinity than adinazolam (Sethy et al 1984). In man, NDMAD is thought to be responsible for benzodiazepine-like effects (sedation, impairment of psychomotor performance and impaired memory) observed after administration of adinazolam (Fleishaker et al 1992a, b).

In the rat and mouse adinazolam is metabolized first to NDMAD; this is subsequently demethylated to didesmethyladinazolam (DDMAD). Deamination of DDMAD results in the formation of a postulated intermediate which undergoes either α-hydroxylation to α-hydroxyalprazolam or cleavage of the side chain to form estazolam (Figure 1; Sethy et al 1984). α-Hydroxyalprazolam and estazolam are the major metabolites in mice. In man, NDMAD is the major metabolite (Sethy et al 1984).

The objective of this study was to investigate the in-vitro metabolism of adinazolam to NDMAD, and of NDMAD to DDMAD, using human liver microsomes and heterologously expressed cytochromes P450 (CYPs) from man. The specific aims were to identify and kinetically characterize the CYP isoforms responsible for the *N*-demethylation of adinazolam and NDMAD. This information should allow more rational forecasting of pharmacokinetic drug–drug interactions and an understanding of the basis of inter-individual variations in drug disposition. Our study suggests that CYP 3A4 is the primary enzyme mediating *N*-demethylation of adinazolam and NDMAD in human liver. This is important information because co-administration of adinazolam with CYP 3A4 inhibitors such as ketoconazole or erythromycin might lead to reduced efficacy because NDMAD is responsible for much of the pharmacological activity of orally administered adinazolam.

Materials and Methods

Materials

Adinazolam, NDMAD, DDMAD, α-hydroxyalprazolam and estazolam were kindly provided by Pharmacia & Upjohn, Kalamazoo, MI. α-Naphthoflavone, sulphaphenazole, omeprazole, quinidine, diethyldithiocarbamate (DDC) and troleandomycin (TAO) were purchased from Sigma (St Louis, MO). Ketoconazole was kindly provided by the Janssen Research Foundation (Beerse, Belgium).

The cofactors $NADP^+$, (±)-isocitric acid, $MgCl_2$ and isocitrate dehydrogenase were purchased from Sigma, as was the KH_2PO_4 salt used in the buffer solution.

Liver samples, obtained from the International Institute for the Advancement of Medicine (Exton, PA), or the Liver Tissue Procurement and Distribution Service (University of Minnesota), were from eight different transplant donors with no history of liver disease. The tissue was partitioned and kept at −80°C until the time of microsome preparation as described previously (von Moltke et al 1993, 1994). Microsomes from cDNA-transfected human lymphoblastoid cells expressing CYP 1A2, 2C9, 2C19, 2D6, 2E1 or 3A4 (Crespi 1995) were purchased from Gentest Corporation (Woburn, MA), divided into samples of suitable size and stored at −80°C; they were thawed on ice before use. Details of microsomal protein concentrations and CYP content were provided by the manufacturer.

Incubation

Incubation mixtures contained potassium phosphate buffer (50 mM; pH 7·5), β-$NADP^+$ (400 μg mL^{-1}), isocitrate dehydrogenase (0·32 units mL^{-1}), $MgCl_2$ (475 μg mL^{-1}) and substrate with or without inhibitor. Final volumes were 0·25 mL, with a microsomal protein concentration of 250–500 μg mL^{-1}. Solutions of adinazolam, NDMAD and the inhibitors were prepared in methanol. The solvent was evaporated to dryness before addition of cofactors.

Substrate, inhibitors, incubation buffer and cofactors were warmed to 37°C, and reactions were initiated by the addition of microsomes. Inhibition studies with α-naphthoflavone, sulphaphenazole, omeprazole, quinidine and ketoconazole were performed by co-incubating inhibitor with substrate, cofactors and microsomes, whereas studies with DDC and TAO were performed by pre-incubating microsomes with inhibitor at 37°C for 20 min before initiation of the reaction. This was because DDC and TAO are mechanism-based inhibitors and require NADPH-dependent complexation to be active (Newton et al 1995). Incubation was performed in a shaking water bath for 20 min at 37°C, then stopped by addition of acetonitrile (100 μL) and cooling on ice. Trazodone (500 ng per tube for studies of adinazolam *N*-demethylation) or antipyrine (250 ng per tube for studies of NDMAD *N*-demethylation) was then added as internal standard and the mixture was centrifuged at 16 000 *g* for 10 min. The supernatant was analysed by high-performance liquid chromatography (HPLC). All incubations were performed in duplicate.

Incubations of adinazolam or NDMAD with microsomes from human lymphoblastoid cells expressing CYP 1A2, 2C9, 2C19, 2D6, 2E1 or 3A4 were performed at 37°C using a protein concentration of 1 mg mL^{-1} and a reaction time of 20 min. Incubation was performed without agitation and with mild shaking only, as recommended by the supplier. Reactions were stopped and products assayed by methods identical with those used for liver microsomal incubations.

Analysis of NDMAD and DDMAD by HPLC

Concentrations of NDMAD or DDMAD were determined by HPLC with ultraviolet detection at 220 nm (Waters Associates, Milford, MA). A 30 cm × 3·9 mm steel C_{18} μBondapak column was used for the separation. The mobile phase was a 22·7 : 77·3 mixture of acetonitrile and 50 mM KH_2PO_4 for determination of NDMAD and a 20 : 80 mixture of the same solvents for determination of DDMAD; the flow rate was 1·1 mL min^{-1}. Standard curves were prepared by adding incubation buffer and internal standard to known amounts of NDMAD or DDMAD to give a final volume of 0·25 mL. Chromatograms were analysed by measurement of peak height using the internal standard method.

Inter-day and intra-day coefficients of variation between duplicate samples were < 6% for the measurement of both NDMAD and DDMAD.

Data analysis

All reaction velocities were based on a 20-min incubation, which falls within the linear time-period for both reactions. Rates were expressed in nanomol min^{-1} (mg protein)$^{-1}$ (in studies using human liver microsomes) or picomol min^{-1} (picomol CYP)$^{-1}$ (in studies using heterologously expressed CYPs). The kinetics of the biotransformations by liver microsomes or cDNA-expressed CYPs were described by either a one-enzyme Michaelis–Menten model:

$$V = V_{max}S/(K_m + S) \quad (1)$$

or a one-enzyme-model Hill equation:

$$V = V_{max}S^A/(K_m^A + S^A) \quad (2)$$

where K_m is the substrate concentration at which the reaction velocity is 50% of the maximum, V_{max}, and A is the Hill coefficient for co-operative substrate binding.

For determination of the inhibition constant (K_i), equation 3, consistent with competitive inhibition according to the Michaelis–Menten equation, was fitted to data points obtained with simultaneously incubated substrate and inhibitor (concentration I):

$$V = V_{max}S/[S + K_m(1 + I/K_i)] \quad (3)$$

V_{max} and K_m were fixed at the values determined by non-linear regression of uninhibited data to equation 1. The iterated variable was K_i, the inhibition constant.

In studies using a fixed concentration of substrate, IC50 values for chemical inhibitors (i.e. the concentration of inhibitor that results in a 50% decrement in reaction velocity) were determined by non-linear regression analysis of data using the equation:

$$R = 100[1 - E_{max}I^A/\{(IC'50)^A + I^A\}] \quad (4)$$

where R is the percentage of the uninhibited reaction velocity that is observed at an inhibitor concentration I, E_{max} is a parameter that describes the extent of maximum inhibition, A is an exponent reflecting the sigmoidicity of the equation, and IC'50 is the apparent IC50 (concentration of inhibitor at which R equals $100 \times [1 - 0{\cdot}5E_{max}]$), from which is calculated the true IC50 by use of the equation:

$$IC50 = IC'50/(2E_{max} - 1)^{1/A} \quad (5)$$

Results

Adinazolam was *N*-demethylated to NDMAD (Figure 2A), and NDMAD to DDMAD (Figure 2B) by human liver microsomes. Incubation of NDMAD also produced appreciable amounts of a yet unidentified metabolite (U) in addition to DDMAD (Figure 2B). On the basis of HPLC retention times this metabolite was neither α-hydroxyalprazolam nor estazolam. The kinetics of adinazolam *N*-demethylation by human liver microsomes could be described by a single-enzyme

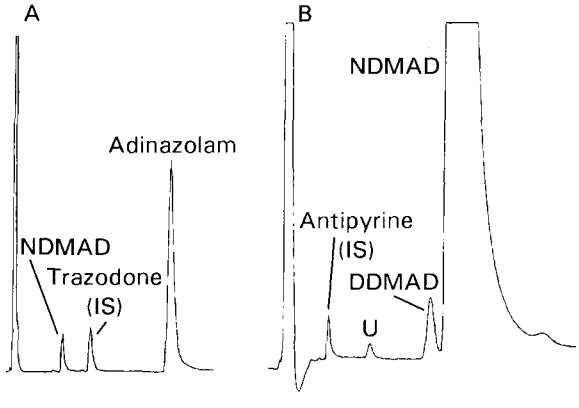

Figure 2. HPLC traces of adinazolam (A) and NDMAD (B) incubated with human liver microsomes (IS = internal standard). For trace A retention times are: NDMAD, 6·6 min; trazodone, 9·7 min; adinazolam, 18·8 min. For trace B retention times are: antipyrine, 6·8 min; U, 11·6 min; DDMAD, 18·5 min; NDMAD 20·7 min.

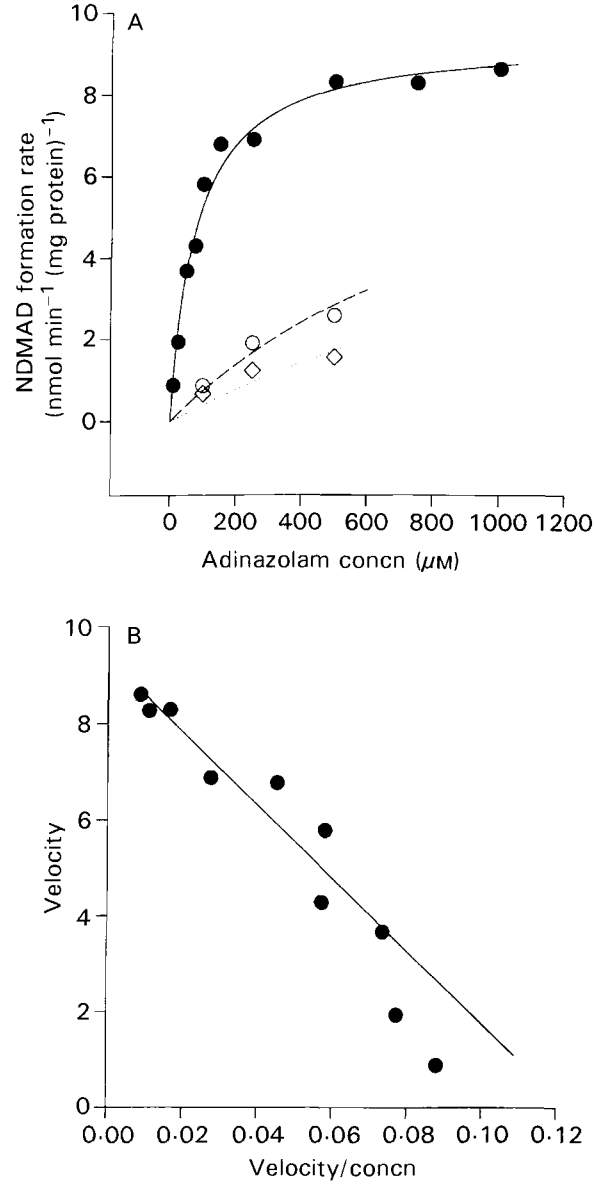

Figure 3. Adinazolam *N*-demethylation by human liver microsomes (liver L4: $V_{max} = 9{\cdot}4$ nmol min^{-1} (mg protein)$^{-1}$, $K_m = 76$ μM, ketoconazole $K_i = 36$ nM). In panel A points are experimental data points; lines are best-fit functions: ●, —, control curve describing the substrate concentration–reaction rate relationship in the absence of inhibitor (equation 1); ○, – – –, reaction velocities when adinazolam was incubated with 0·5 μM ketoconazole; ◇, · · ·, reaction velocities when adinazolam was incubated with 1 μM ketoconazole. Panel B shows an Eadie-Hofstee plot of adinazolam *N*-demethylation by human liver microsomes. Points are experimental data points; the line is the fitted function.

Michaelis–Menten model (equation 1; Figure 3, Table 1). In three of the four livers studied substrate activation was evident in the kinetics of formation of DDMAD and U from NDMAD. A Hill enzyme-model was thus fitted to the data (equation 2; Figure 4, Table 2).

Adinazolam was demethylated by microsomes from cDNA-transfected lymphoblastoid cells from

Table 1. Kinetic parameters and ketoconazole inhibition constants for adinazolam *N*-demethylation in six different human liver microsomal preparations.

Parameter	Liver sample						Mean*	s.d.†
	L1	L2	L3	L4	L5	L6		
V_{max} (nmol min^{-1} (mg protein)$^{-1}$)	3·85	8·17	3·42	9·36	6·78	1·31	5·48	3·1
K_m (μM)	103·8	98·2	80·3	76·1	74·6	117·6	91·8	17·5
V_{max}/K_m (μL min^{-1} (mg protein)$^{-1}$)	37·1	83·2	42·6	123	90·9	11·1	64·7	41·4
K_i (nM)	28·4	34·7	19·4	35·6	32·7	650	30·2‡	6·6‡

*Arithmetic mean. † Standard deviation. ‡ With K_i for liver L6 excluded.

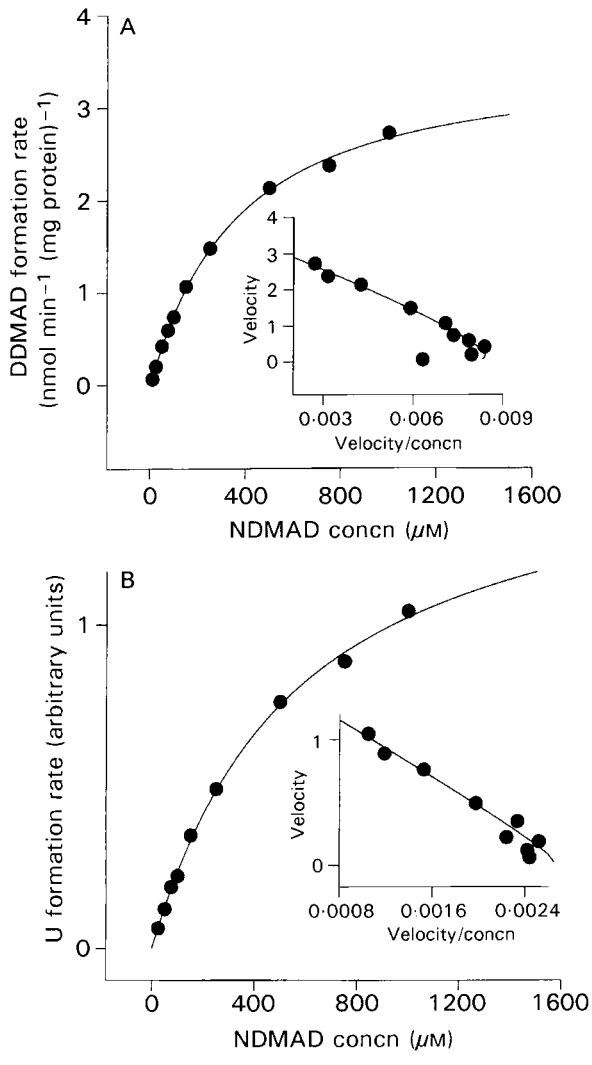

Figure 4. *N*-demethylation (A), and formation of U (B) from NDMAD by human liver microsomes (liver L2). Kinetic parameters for this liver for formation of DDMAD are: $V_{max} = 3·5$ nmol min^{-1} (mg protein)$^{-1}$, $K_m = 345$ μM, and Hill number A = 1·05. Parameters for formation of U are: $K_m = 551$ μM, and Hill number A = 1·02. ●, Experimental data points; —, the fitted Hill enzyme function (equation 2). The insets are Eadie-Hofstee plots with experimental data points and fitted functions.

man expressing CYPs 3A4 and 2C19; no activity was detected for CYPs 1A2, 2C9, 2D6 and 2E1. Model parameters indicated that CYP 2C19 had high affinity (low K_m) and low capacity (low V_{max}) for adinazolam *N*-demethylation (Figure 5, Table 3) whereas CYP 3A4 had low affinity (high K_m) and high capacity (high V_{max}). NDMAD was *N*-demethylated to DDMAD by CYPs 3A4, 2C19, 2C9 and 1A2; no activity was detected for CYPs 2D6 and 2E1. Substrate activation (Hill enzyme kinetics) was evident in the kinetics of NDMAD *N*-demethylation by CYPs 3A4 and 2C19 but not by CYP 2C9. Model parameters indicated that CYP 2C19 and CYP 3A4 had high affinity (low K_m) and high capacity (high V_{max}) for NDMAD *N*-demethylation whereas CYP 2C9 showed low affinity (high K_m) and low capacity (low V_{max}) (Figure 6A, Table 4). The kinetics of NDMAD *N*-demethylation by CYP 1A2 were not studied because the rate of reaction at a substrate concentration of 250 μM was two orders of magnitude lower than that with CYP 3A4. The metabolite U was produced from NDMAD by CYP 3A4 only, and the kinetics were consistent with a Hill enzyme-model, suggesting substrate activation (K_m 128 ± 16 μM, Hill number A 1·72 ± 0·3; mean ± s.e.m.) (Figure 6B).

Adinazolam *N*-demethylation was strongly inhibited by ketoconazole, a relatively specific CYP 3A4 inhibitor. In five of six livers tested, the K_i for ketoconazole inhibition of adinazolam *N*-demethylation was < 40 nM, suggesting that CYP 3A4 is a major adinazolam *N*-demethylase. In one liver known to be low in CYP 3A4 activity (L6), the K_i for ketoconazole was 650 nM (Table 1). More than 90% of adinazolam *N*-demethylation activity was abolished by 1–2·5 μM ketoconazole for both 10 μM and 100 μM concentrations of adinazolam (Figure 7A). At both substrate concentrations, the IC50 for ketoconazole inhibition of adinazolam *N*-demethylation was 0·15 μM (n = 4). TAO (0·5–25 μM), a CYP 3A4-specific inhibitor,

Table 2. Kinetic parameters for *N*-desmethyladinazolam metabolism in four different human liver microsomal preparations.

Parameter	Liver sample				Mean*	s.d.†
	L2	L5	L7	L8		
V_{max} (nmol min^{-1} (mg protein)$^{-1}$)	3·54	2·38	2·69	0·632	2·31	1·2
K_m (μM)	344·8	208·6	230·7	252·3	259·1	60
Hill number for formation of didesmethyladinazolam	1·05	1·13	1·19	1·0	1·09	0·08
V_{max}/K_m (μL min^{-1} (mg protein)$^{-1}$)	10·3	11·4	11·7	2·5	8·98	4·4
Concentration of *N*-desmethyladinazolam at which the reaction velocity of formation of U is 50% of the maximum (μM)	551	311	367	764	498·4	205
Hill number for formation of U	1·02	1·22	1·27	1·0	1·13	0·14

*Arithmetic mean. † Standard deviation.

inhibited adinazolam *N*-demethylation in a concentration-dependent manner (Figure 7B) with maximum inhibition of 79·1 ± 4·5% and an IC50 of 1·96 ± 0·4 μM (n = 4; mean ± s.e.m.). The incomplete inhibition of adinazolam *N*-demethylation by TAO is in agreement with earlier reports on the effect of this inhibitor on CYP 3A4-mediated reactions (Newton et al 1995).

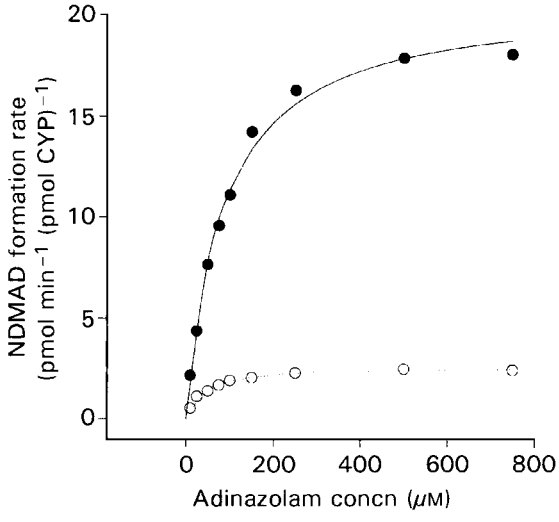

Figure 5. Adinazolam *N*-demethylation by cDNA-expressed CYPs 2C19 (○, ···) and 3A4 (●, —). The symbols are experimental data points and the lines are curves fitted to a single-enzyme Michaelis–Menten model (equation 1). See Table 3 for kinetic parameters.

Omeprazole, a relatively specific CYP 2C19 inhibitor at concentrations up to 10 μM (Ko et al 1997), inhibited adinazolam *N*-demethylation in a concentration-dependent manner (Figure 7C), at both 10 μM and 100 μM concentrations of adinazolam (IC50 = 21 ± 5 μM (mean ± s.e.m., n = 4) at a substrate concentration of 100 μM). At omeprazole concentrations greater than 10 μM, inhibition was greater at 100 μM adinazolam than at 10 μM adinazolam. However, at these concentrations, omeprazole inhibits CYP 2C9, 3A4 and 2C19 (Ko et al 1997). The approximately 30% decrement in reaction velocity produced by 10 μM omeprazole at either substrate concentration suggests that CYP 2C19 might play a significant although minor role in adinazolam *N*-demethylation.

α-Naphthoflavone (up to 0·5 μM), sulphaphenazole (up to 10 μM), quinidine (up to 100 μM) and DDC (up to 500 μM) did not inhibit adinazolam *N*-demethylation, confirming the inference of a lack of a quantitatively important role for CYPs 1A2, 2C9, 2D6 and 2E1 in this reaction.

Formation of both DDMAD and U from NDMAD was strongly inhibited by ketoconazole (Figure 8). At a substrate concentration of 250 μM, the IC50 for ketoconazole inhibition of NDMAD *N*-demethylation was 0·14 ± 0·04 μM (n = 4, mean ± s.e.m.). The IC50 for ketoconazole inhibition of the formation of U from NDMAD was < 0·1 μM (the exact value could not be com-

Table 3. Kinetic parameters for adinazolam *N*-demethylation by cDNA-expressed human CYPs.

Parameter	CYP 2C19	CYP 3A4
V_{max} (pmol min^{-1} (pmol CYP)$^{-1}$)	2·61 ± 0·04	20·8 ± 0·5
K_m (μM)	39·1 ± 2·5	83·4 ± 6·3
V_{max}/K_m (intrinsic clearance) (nL min^{-1} (pmol CYP)$^{-1}$)	66·6	249·5
Abundance-adjusted intrinsic clearance†	3·1	96·9

* Means ± s.e.m. † Intrinsic clearance multiplied by the relative abundance of the CYP isoform in human liver expressed in percent.

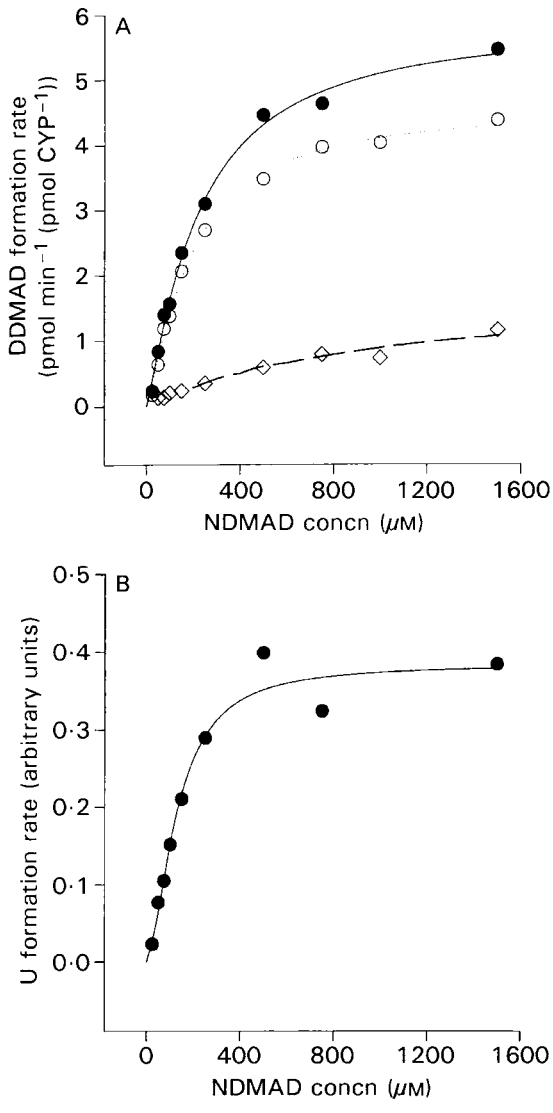

Figure 6. A. NDMAD *N*-demethylation by cDNA-expressed CYPs 2C9 (◇, – –), 2C19 (○, · · ·) and 3A4 (●, —). B. Formation of U from NDMAD by cDNA-expressed CYP 3A4. The symbols are experimental data points and the lines are curves fitted to a single-enzyme Michaelis–Menten model (equation 1) for CYP 2C9, or a Hill enzyme-model (equation 2) for CYP 2C19 and CYP 3A4. See Table 4 for kinetic parameters.

puted because there was 100% inhibition by 0·5–1 μM ketoconazole). Sulphaphenazole did not significantly inhibit the production of either DDMAD or U from NDMAD at a substrate concentration of 250 μM, indicating the lack of a quantitatively important role for CYP 2C9 in NDMAD metabolism. Omeprazole at concentrations up to 10 μM (at which it is relatively specific to CYP 2C19) did not significantly inhibit NDMAD *N*-demethylation, indicating the lack of a quantitatively important role for CYP 2C19 in NDMAD *N*-demethylation.

Discussion

Previous studies on adinazolam have mainly focused on the pharmacokinetics of the drug and its metabolite NDMAD in man, and the relationship between the plasma concentrations of adinazolam and NDMAD and the pharmacodynamic effects. Given that NDMAD is an active metabolite and might account for most of the pharmacological activity of orally administered adinazolam, it is important that factors regulating the hepatic biotransformation of adinazolam to NDMAD be understood, because inhibition or induction of adinazolam *N*-demethylation might result in a diminished or enhanced effect, respectively. We have used in-vitro techniques to investigate the kinetics of adinazolam metabolism by human liver microsomes. Adinazolam *N*-demethylation is described by a single-enzyme Michaelis–Menten enzyme kinetic model. By use of microsomes from lymphoblastoid cells expressing human CYPs, we conclude that CYPs 3A4 and 2C19 can *N*-demethylate adinazolam. In human liver, CYPs 1A2, 2C, 2D6 and 3A on average account for 12·7, 18·2, 1·5 and 28·8%, respectively, of total hepatic microsomal CYP (Shimada et al 1994). Adjusting the reaction rates observed with cDNA-expressed human CYPs for these average values of relative abundance of the CYPs in the liver in man yields the picture shown in Figure 9. It has been suggested that in man CYP 2C9 is the most mass-abundant

Table 4. Kinetic parameters for *N*-demethylation of *N*-desmethyladinazolam by cDNA-expressed human CYPs.

Parameter	CYP 2C9	CYP 2C19	CYP 3A4
V_{max} (pmol min^{-1} (pmol CYP)$^{-1}$)	1·85 ± 0·3*	4·58 ± 0·14*	5·9 ± 0·25*
K_m (μM)	1068 ± 330*	187·1 ± 14*	220 ± 22*
Hill number A	–†	1·29 ± 0·09	1·21 ± 0·09
V_{max}/K_m (intrinsic clearance) (nL min^{-1} (pmol CYP)$^{-1}$)	1·7	24·5	26·9
Abundance-adjusted intrinsic clearance‡	2·8	9·7	87·5

* Mean ± s.e.m. † No sigmoidicity was evident and a one-enzyme Michaelis–Menten model was used.
‡ Intrinsic clearance multiplied by the relative abundance of the CYP isoform in human liver, in percent.

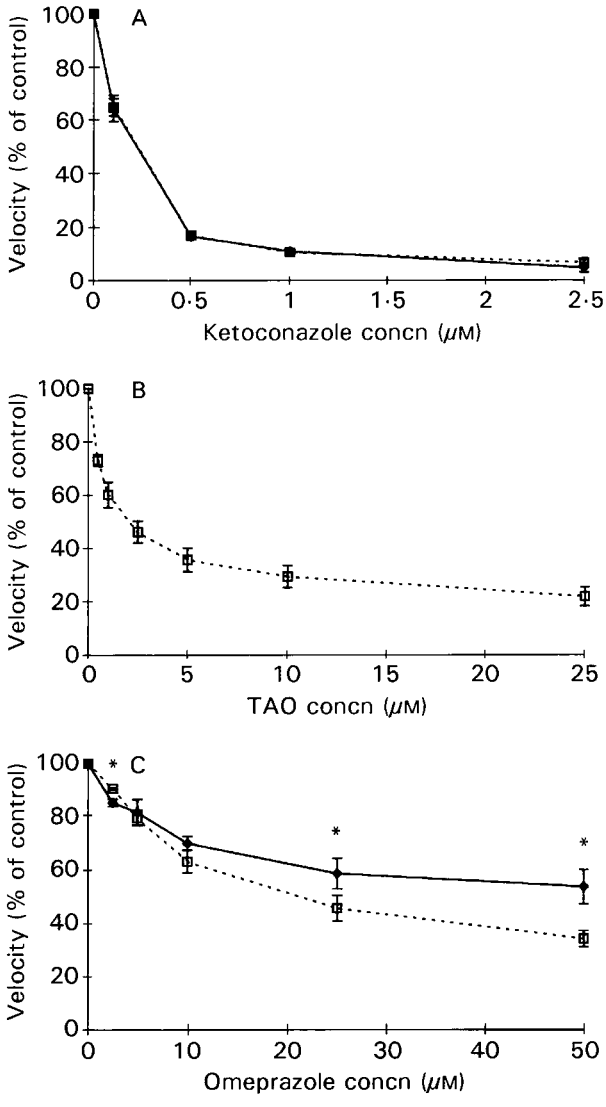

Figure 7. Effect of ketoconazole (A), TAO (B) and omeprazole (C) on adinazolam *N*-demethylation by human liver microsomes for adinazolam concentrations of 10 μM (◆, —) and 100 μM (□, – –) . Points represent the amount (%) of control activity and are means ± s.e.m. of results from four microsomal preparations. *$P < 0.05$, amount of control activity remaining when 10 μM adinazolam was used was significantly different from that remaining when 100 μM adinazolam was used, for that particular concentration of inhibitor. TAO inhibition data are for a substrate concentration of 100 μM.

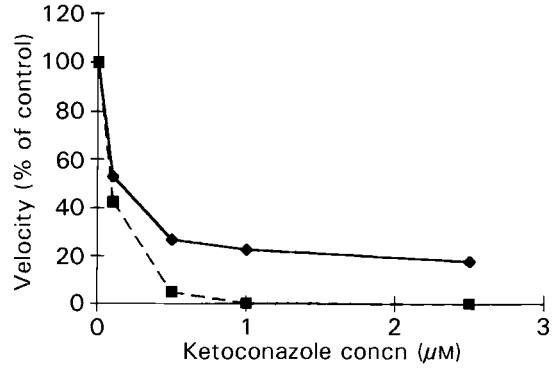

Figure 8. Effect of ketoconazole on the formation of DDMAD (◆, —) and U (■, – –) from NDMAD (250 μM) by human liver microsomes. Points represent the amount (%) of control activity. Results are means ± s.e.m. of results from four microsomal preparations.

CYP 2C isoform in human liver (Crespi 1995) but the relative abundance of these two CYP 2C isoforms in human liver is not yet known. We have determined the ratio of the relative activity factors (Crespi 1995) for CYP 2C9 and CYP 2C19 to be 4·26 ± 1·55 (mean ± s.e.m., n = 10) using cDNA-expressed CYPs 2C9 and 2C19, and human liver microsomes from our liver bank (Venkatakrishnan et al, unpublished results). Because we utilized the same expression system (human lymphoblastoid cells) for CYP 2C9 and 2C19, the ratio of relative activity factors should reflect the ratio of the abundance of these two isoforms in the liver in man. On the basis of this assumption, CYP 2C9 and 2C19 should account for 14·7 and 3·5%, respectively, of total hepatic microsomal CYP. Figure 9 should best describe the situation in human liver microsomes, and indicates that CYP 3A4 is the primary enzyme mediating adinazolam *N*-demethylation at all substrate concentrations. Thus, although the intrinsic clearance of adinazolam *N*-demethylation by CYP 3A4 is only 3·7 times that by CYP 2C19 (Table 3), the abundance-adjusted intrinsic clearances for the two isoforms suggest that in man only 3% of adinazolam *N*-demethylation activity in the liver is contributed by CYP 2C19, with CYP 3A4 accounting for 97% of the net intrinsic clearance (Table 3). This is consistent with the high susceptibility to inhibition by ketoconazole. However, the extent of inhibition of adinazolam *N*-demethylation by 10 μM omeprazole in human liver microsomes is somewhat greater than predicted by this model. This is probably explained by the relative rather than absolute specificity of omeprazole as an inhibitor of CYP 2C19. Although omeprazole is a relatively specific CYP 2C19 inhibitor at a concentration of 10 μM (Ko et al 1997), it may not be absolutely specific; this might explain the discrepancy. Given that CYP 3A4 is a high-abundance high-capacity adinazolam *N*-demethylase, even a small amount of CYP 3A4 inhibition by omeprazole can result in significant inhibition of adinazolam *N*-demethylation by liver microsomes. Thus, although CYP 2C19 has catalytic activity as an adinazolam *N*-demethylase, CYP 3A4 is the primary enzyme mediating this pathway in human liver.

NDMAD was demethylated to DDMAD by human liver microsomes, and by cDNA-expressed CYPs 3A4, 2C19, 2C9 and 1A2. Substrate activation was observed in three of four livers studied.

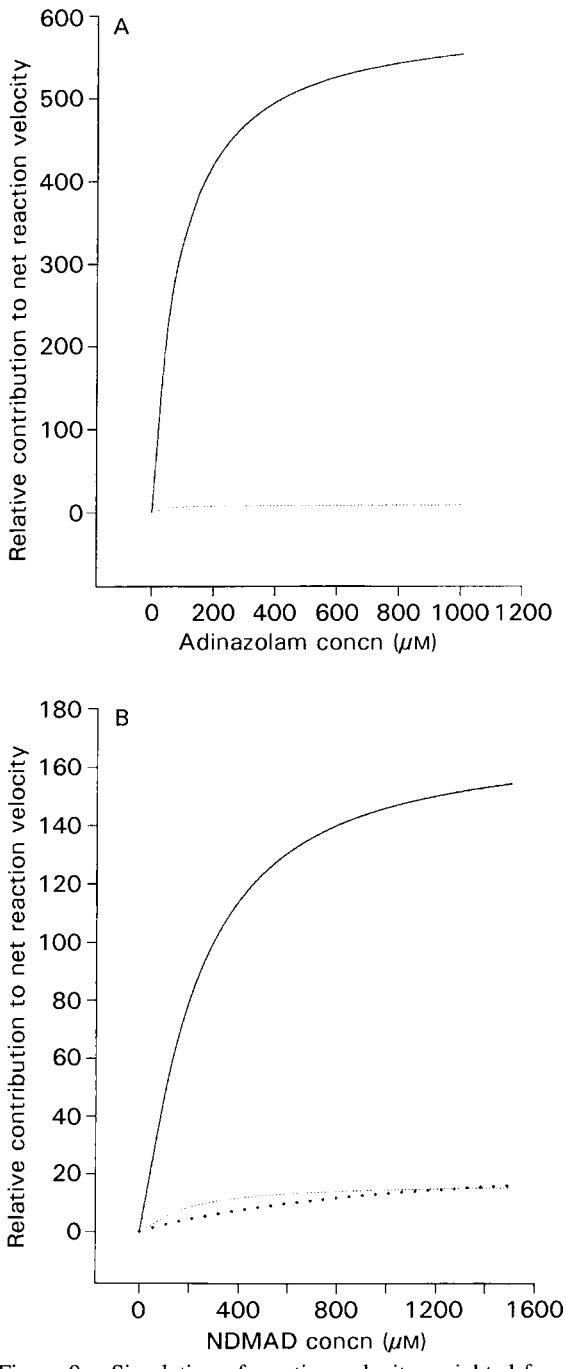

Figure 9. Simulation of reaction velocity weighted for relative abundance as a function of substrate concentration for the CYP enzymes mediating adinazolam *N*-demethylation (A) and NDMAD *N*-demethylation (B): —, function for CYP 3A4; ···, function for CYP 2C19; · · ·, function for CYP 2C9.

Thus a Hill enzyme-model was used to describe NDMAD *N*-demethylation by human liver microsomes. Although substrate activation was observed in the kinetics of NDMAD *N*-demethylation by CYPs 3A4 and 2C19, hyperbolic kinetics consistent with a one-enzyme Michaelis–Menten model were observed for NDMAD *N*-demethylation by CYP 2C9. Substrate activation was also evident in the kinetics of formation of an unidentified metabolite U from NDMAD by CYP 3A4. Sigmoidal enzyme kinetics have been observed for many CYP 3A4-catalysed reactions (Schmider et al 1995; Ueng et al 1997) and is suggestive of co-operative substrate binding. As with adinazolam, CYP 3A4 was identified by chemical inhibition experiments as the major NDMAD *N*-demethylase. Omeprazole at a concentration of 10 μM did not significantly inhibit NDMAD demethylation rates at a substrate concentration of 250 μM. This is consistent with a contribution of CYP 2C19 to the net NDMAD demethylation rate of < 10% at a substrate concentration of 250 μM, as inferred from abundance-corrected kinetics of NDMAD *N*-demethylation by cDNA-expressed CYPs (Figure 9B). Thus, although the intrinsic clearance for NDMAD *N*-demethylation by CYP 2C19 is only slightly smaller than for that by CYP 3A4 (Table 4), adjusting these values for the relative abundance of the enzymes in the liver in humans suggests that CYP 3A4 is the primary NDMAD *N*-demethylase contributing to 87·5% of the net intrinsic clearance (Table 4) with CYPs 2C19 and CYP 2C9 playing relatively minor roles. Lack of a quantitatively important role for CYP 2C9 in NDMAD *N*-demethylation is supported both by lack of inhibition by sulphaphenazole, and by the abundance-corrected predicted contribution of CYP 2C9 (Figure 9B, Table 4).

In addition to DDMAD, human liver microsomes produced appreciable amounts of another unidentified metabolite U. In mice and rats DDMAD is deaminated to a postulated intermediate which undergoes either α-hydroxylation to form α-hydroxyalprazolam or cleavage of the side chain to form estazolam (Figure 1; Sethy et al 1984). The metabolite U formed by human liver microsomes, however, was neither α-hydroxyalprazolam nor estazolam since its HPLC retention time did not match that of either compound. Formation of U from NDMAD is mediated by cDNA-expressed CYP 3A4 only. This is consistent with complete inhibition of the reaction in human liver microsomes by 1 μM ketoconazole.

Both adinazolam and NDMAD are primarily metabolized by CYP 3A4 in human liver microsomes. However, CYP 3A4 is also present in the small intestine, and might account for a substantial fraction of the pre-systemic extraction of orally administered adinazolam. NDMAD is cleared mainly by a renal route, with greater than 60% of the dose of intravenously administered adinazolam or NDMAD appearing as NDMAD in the urine (Fleishaker et al 1992b). Thus, hepatic metabolism to DDMAD might play a minor role in NDMAD clearance. This is also consistent with nearly an

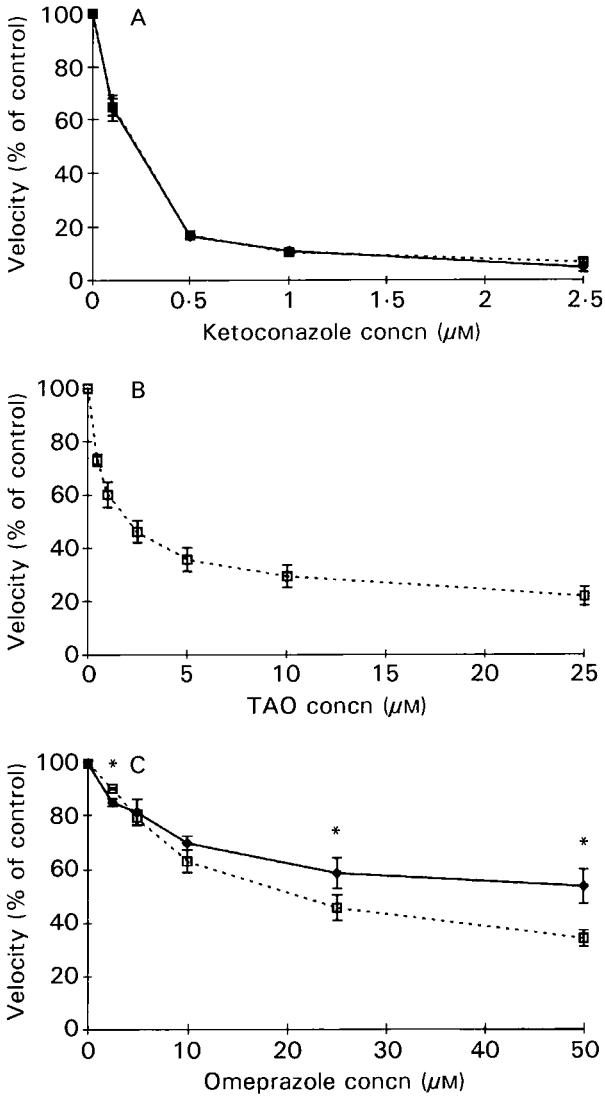

Figure 7. Effect of ketoconazole (A), TAO (B) and omeprazole (C) on adinazolam *N*-demethylation by human liver microsomes for adinazolam concentrations of 10 μM (◆, —) and 100 μM (□, – –) . Points represent the amount (%) of control activity and are means ± s.e.m. of results from four microsomal preparations. *$P < 0.05$, amount of control activity remaining when 10 μM adinazolam was used was significantly different from that remaining when 100 μM adinazolam was used, for that particular concentration of inhibitor. TAO inhibition data are for a substrate concentration of 100 μM.

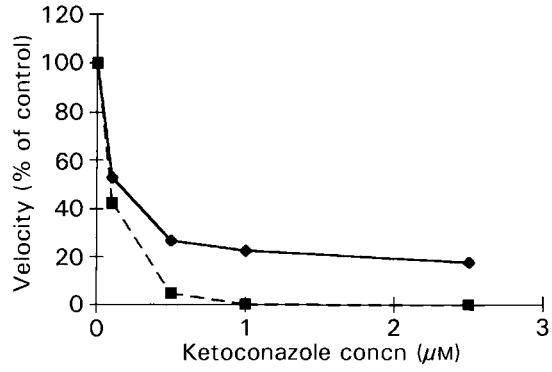

Figure 8. Effect of ketoconazole on the formation of DDMAD (◆, —) and U (■, – –) from NDMAD (250 μM) by human liver microsomes. Points represent the amount (%) of control activity. Results are means ± s.e.m. of results from four microsomal preparations.

CYP 2C isoform in human liver (Crespi 1995) but the relative abundance of these two CYP 2C isoforms in human liver is not yet known. We have determined the ratio of the relative activity factors (Crespi 1995) for CYP 2C9 and CYP 2C19 to be 4·26 ± 1·55 (mean ± s.e.m., n = 10) using cDNA-expressed CYPs 2C9 and 2C19, and human liver microsomes from our liver bank (Venkatakrishnan et al, unpublished results). Because we utilized the same expression system (human lymphoblastoid cells) for CYP 2C9 and 2C19, the ratio of relative activity factors should reflect the ratio of the abundance of these two isoforms in the liver in man. On the basis of this assumption, CYP 2C9 and 2C19 should account for 14·7 and 3·5%, respectively, of total hepatic microsomal CYP. Figure 9 should best describe the situation in human liver microsomes, and indicates that CYP 3A4 is the primary enzyme mediating adinazolam *N*-demethylation at all substrate concentrations. Thus, although the intrinsic clearance of adinazolam *N*-demethylation by CYP 3A4 is only 3·7 times that by CYP 2C19 (Table 3), the abundance-adjusted intrinsic clearances for the two isoforms suggest that in man only 3% of adinazolam *N*-demethylation activity in the liver is contributed by CYP 2C19, with CYP 3A4 accounting for 97% of the net intrinsic clearance (Table 3). This is consistent with the high susceptibility to inhibition by ketoconazole. However, the extent of inhibition of adinazolam *N*-demethylation by 10 μM omeprazole in human liver microsomes is somewhat greater than predicted by this model. This is probably explained by the relative rather than absolute specificity of omeprazole as an inhibitor of CYP 2C19. Although omeprazole is a relatively specific CYP 2C19 inhibitor at a concentration of 10 μM (Ko et al 1997), it may not be absolutely specific; this might explain the discrepancy. Given that CYP 3A4 is a high-abundance high-capacity adinazolam *N*-demethylase, even a small amount of CYP 3A4 inhibition by omeprazole can result in significant inhibition of adinazolam *N*-demethylation by liver microsomes. Thus, although CYP 2C19 has catalytic activity as an adinazolam *N*-demethylase, CYP 3A4 is the primary enzyme mediating this pathway in human liver.

NDMAD was demethylated to DDMAD by human liver microsomes, and by cDNA-expressed CYPs 3A4, 2C19, 2C9 and 1A2. Substrate activation was observed in three of four livers studied.

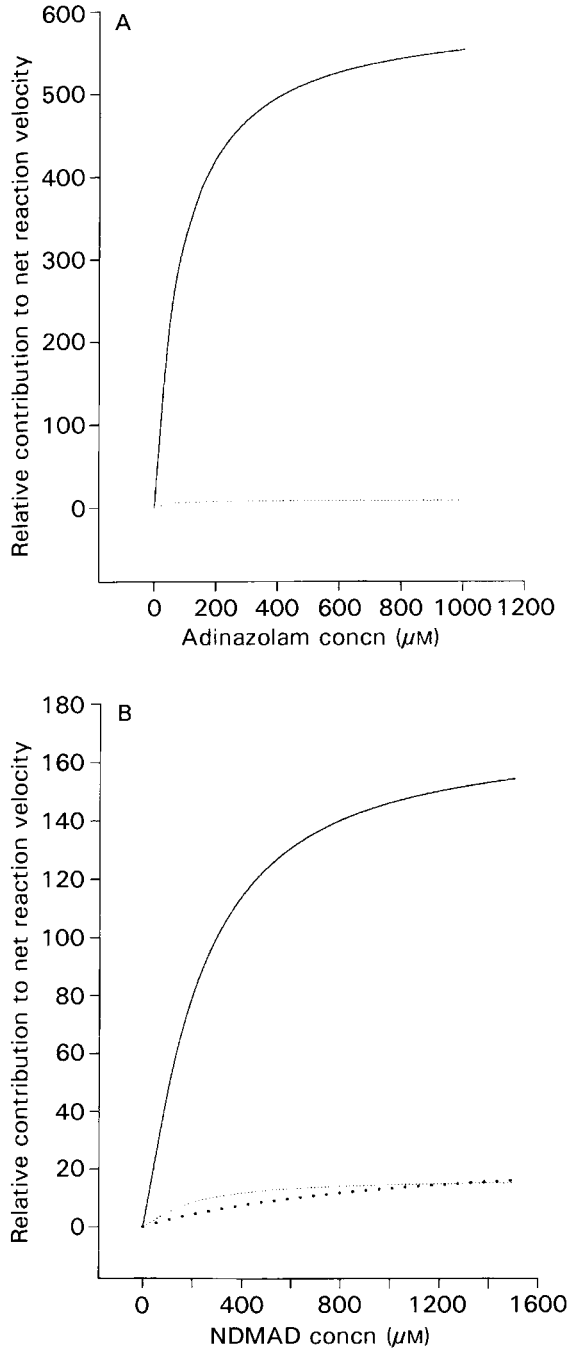

Figure 9. Simulation of reaction velocity weighted for relative abundance as a function of substrate concentration for the CYP enzymes mediating adinazolam *N*-demethylation (A) and NDMAD *N*-demethylation (B): —, function for CYP 3A4; ···, function for CYP 2C19; · · ·, function for CYP 2C9.

Thus a Hill enzyme-model was used to describe NDMAD *N*-demethylation by human liver microsomes. Although substrate activation was observed in the kinetics of NDMAD *N*-demethylation by CYPs 3A4 and 2C19, hyperbolic kinetics consistent with a one-enzyme Michaelis–Menten model were observed for NDMAD *N*-demethylation by CYP 2C9. Substrate activation was also evident in the kinetics of formation of an unidentified metabolite U from NDMAD by CYP 3A4. Sigmoidal enzyme kinetics have been observed for many CYP 3A4-catalysed reactions (Schmider et al 1995; Ueng et al 1997) and is suggestive of co-operative substrate binding. As with adinazolam, CYP 3A4 was identified by chemical inhibition experiments as the major NDMAD *N*-demethylase. Omeprazole at a concentration of 10 μM did not significantly inhibit NDMAD demethylation rates at a substrate concentration of 250 μM. This is consistent with a contribution of CYP 2C19 to the net NDMAD demethylation rate of $< 10\%$ at a substrate concentration of 250 μM, as inferred from abundance-corrected kinetics of NDMAD *N*-demethylation by cDNA-expressed CYPs (Figure 9B). Thus, although the intrinsic clearance for NDMAD *N*-demethylation by CYP 2C19 is only slightly smaller than for that by CYP 3A4 (Table 4), adjusting these values for the relative abundance of the enzymes in the liver in humans suggests that CYP 3A4 is the primary NDMAD *N*-demethylase contributing to 87·5% of the net intrinsic clearance (Table 4) with CYPs 2C19 and CYP 2C9 playing relatively minor roles. Lack of a quantitatively important role for CYP 2C9 in NDMAD *N*-demethylation is supported both by lack of inhibition by sulphaphenazole, and by the abundance-corrected predicted contribution of CYP 2C9 (Figure 9B, Table 4).

In addition to DDMAD, human liver microsomes produced appreciable amounts of another unidentified metabolite U. In mice and rats DDMAD is deaminated to a postulated intermediate which undergoes either α-hydroxylation to form α-hydroxyalprazolam or cleavage of the side chain to form estazolam (Figure 1; Sethy et al 1984). The metabolite U formed by human liver microsomes, however, was neither α-hydroxyalprazolam nor estazolam since its HPLC retention time did not match that of either compound. Formation of U from NDMAD is mediated by cDNA-expressed CYP 3A4 only. This is consistent with complete inhibition of the reaction in human liver microsomes by 1 μM ketoconazole.

Both adinazolam and NDMAD are primarily metabolized by CYP 3A4 in human liver microsomes. However, CYP 3A4 is also present in the small intestine, and might account for a substantial fraction of the pre-systemic extraction of orally administered adinazolam. NDMAD is cleared mainly by a renal route, with greater than 60% of the dose of intravenously administered adinazolam or NDMAD appearing as NDMAD in the urine (Fleishaker et al 1992b). Thus, hepatic metabolism to DDMAD might play a minor role in NDMAD clearance. This is also consistent with nearly an

order of magnitude lower intrinsic clearance of NDMAD by *N*-demethylation in comparison with adinazolam *N*-demethylation by human liver microsomes (Tables 1 and 2). Inhibition of CYP 3A4 by co-administration of drugs such as ketoconazole or erythromycin might thus lead to reduced efficacy, because much of the pharmacological activity of adinazolam is attributable to NDMAD.

Acknowledgements

The work was supported by grants MH-34223, DA-05258, MH-19924 and RR-00054 from the Department of Health and Human Services. Dr von Moltke is the recipient of a Scientist Development Award (K21-MH-01237) from the National Institute of Mental Health.

References

Crespi, C. L. (1995) Xenobiotic-metabolizing human cells as tools for pharmacological and toxicological research. Adv. Drug Res. 26: 179–235

Fleishaker, J. C., Phillips, J. P. (1989) Adinazolam pharmacokinetics and behavioral effects following administration of 20–60 mg doses of its mesylate salt in healthy volunteers. Psychopharmacology 99: 34–39

Fleishaker, J. C., Smith, T. C., Friedman, H. L., Hulst, L. K. (1992a) Separation of the pharmacokinetic/pharmacodynamic properties of oral and i.v. adinazolam mesylate and *N*-desmethyladinazolam mesylate in healthy volunteers. Drug Invest. 4: 155–165

Fleishaker, J. C., Hulst, L. K., Smith, T. C., Friedman, H. L. (1992b) Clinical pharmacology of adinazolam and *N*-desmethyladinazolam mesylate following single intravenous infusions of each compound in healthy volunteers. Eur. J. Clin. Pharmacol. 42: 287–294

Ko, J.-W., Sukhowa, N., Thacker, D., Chen, P., Flockhart, D. A. (1997) Evaluation of omeprazole and lansoprazole as inhibitors of cytochrome P450 isoforms. Drug Metab. Dispos. 25: 853–862

Newton, D. J., Wang, R. W., Lu, A. Y. H. (1995) Cytochrome P450 inhibitors. Evaluation of specificities in the in vitro metabolism of therapeutic agents by human liver microsomes. Drug Metab. Dispos. 23: 154–158

Schmider, J., Greenblatt, D. J., von Moltke, L. L., Harmatz, J. S., Shader, R. I. (1995) *N*-Demethylation of amitriptyline in vitro: role of cytochrome P-450 3A (CYP3A) isoforms and effect of metabolic inhibitors. J. Pharmacol. Exp. Ther. 275: 592–597

Sethy, V. H., Collins, R. J., Daniels, E. G. (1984) Determination of biological activity of adinazolam and its metabolites. J. Pharm. Pharmacol. 36: 546–548

Shimada, T., Yamazaki, S., Mimura, M., Inui, Y., Guengerich, F. P. (1994) Interindividual variations in human liver cytochrome P-450 enzymes involved in the oxidation of drugs, carcinogens and toxic chemicals: studies with liver microsomes of 30 Japanese and 30 Caucasians. J. Pharmacol. Exp. Ther. 270: 414–423

Ueng, Y.-F., Kuwabara, T., Chun, Y.-J., Guengerich, F. P. (1997) Cooperativity in oxidations catalysed by cytochrome P450 3A4. Biochemistry 36: 370–381

von Moltke, L. L., Greenblatt, D. J., Harmatz, J. S., Shader, R. I. (1993) Alprazolam metabolism in vitro: studies of human, monkey, mouse, and rat liver microsomes. Pharmacology 47: 268–276

von Moltke, L. L., Greenblatt, D. J., Cotreau-Bibbo, M. M., Duan, S. X., Harmatz, J. S., Shader, R. I. (1994) Inhibition of desipramine hydroxylation in vitro by serotonin reuptake inhibitor antidepressants, and by quinidine and ketoconazole: a model system to predict drug interaction in vivo. J. Pharmacol. Exp. Ther. 268: 1278–1283